J Appl Electrochem (2014) 44:1179–1184
DOI 10.1007/s10800-014-0734-7

RESEARCH ARTICLE

Preparing a catalyst layer in magnetic field to improve the performance of proton exchange membrane fuel cells

Xin Sun · Hongfeng Xu · Lu Lu · Wangyan Xing · Hong Zhao

Received: 19 May 2014 / Accepted: 18 August 2014 / Published online: 26 August 2014

Abstract Electro catalyst Pt–Co/multi-walled C nanotubes were synthesized by using the modified polyol method with glycol as reducer. The magnetic-field-assisted fabrication of membrane electrode assemblies (MEAs) for proton exchange membrane fuel cells (PEMFCs) was proposed, to orient catalyst layers and increase the efficiency of catalyst utilization. PEMFCs with the magnetic-field-treated MEA (M-MEA) exhibited significant performance improvement over common MEA (C-MEA) without magnetic-field treatment. Under the same operating conditions, the maximum power density of MEA increased from 149.6 to 223.8 mW cm^{-2} when C-MEA was replaced by M-MEA. Scanning electron microscope images showed that catalysts exhibited a "cluster-like structure" in M-MEA opposed to a chaotic arrangement in C-MEA. Electrochemical impedance spectroscopy measurements revealed that M-MEA reaction resistance was lower than that of C-MEA. Cyclic voltammetry data showed an increment of almost 29.6 % in electrochemical surface area as a result of the magnetic-field treatment.

Keywords PEMFCs · Magnetic field · Performance · Pt–Co/MWCNT

X. Sun · H. Xu (✉) · L. Lu · W. Xing · H. Zhao
Liaoning Province Key Laboratory for New Energy Battery, Dalian Jiaotong University, 794 Huanghe Road, Dalian 116028, People's Republic of China
e-mail: hfxu@fuelcell.com.cn

X. Sun
e-mail: fei-kebi@163.com

1 Introduction

Proton exchange membrane fuel cells (PEMFCs) have recently attracted increasing attention as alternative mobile and portable power sources for such outstanding advantages as high efficiency, high power density, low or zero emissions, and reliability [1–3]. A key component of PEMFCs is the membrane electrode assembly (MEA), which consists of a proton exchange membrane, such as a Nafion membrane, sandwiched between two catalyst layers that serve as anodic and cathodic electrodes.

Considerable efforts have been exerted to optimize MEA electrode composition and structure to extend the effective utilization of catalysts and decrease cost. Alloying Pt with transition metals, such as Co, Fe, and Ni, is an efficient mean to enhance catalytic activity for the oxygen reduction reaction through the formation of a new electronic structure; this process shortens the Pt–Pt distance to favor the adsorption of O molecules [4–7]. To achieve high activity, Pt particle size should be uniformly dispersed and controlled on area supports [8–10]. High-surface area electro catalyst support materials are important in uniformly dispersing electro catalyst nanoparticles to reduce electro catalyst loading and improve fuel cell performance. Thus, multi-walled C nanotubes (MWCNTs) appear to be ideal candidates for use as electro catalyst support material because of their large surface area, good thermal and chemical stability, and high electrical conductivity [11, 12]. Earlier studies have been focused on MWCNT catalyst layer composition.

Particles tend to form "pearl-chains" under the influence of an electric field. Although a few studies have been conducted on the preparation of aligned or oriented structures in various conductive membranes with an electric field as the driving force [13–17], Middelman [18] was the

first to report on the fabrication of oriented MEA electrodes for PEMFCs by using an electric field. The application of strong magnetic fields on materials induces strong magnetic-field effects. Such effects can result in the creation of highly functional nanomaterials with new properties, which result from the new interfaces or nanostructures formed by the strong magnetic fields [19]. Hasanabadi [20] reported that γ-Fe_2O_3 nanoparticles aligned across the membrane when a magnetic field is applied. Anisotropic nanocomposite membranes with oriented nanoparticles have potential application in fuel cells. Wang [21] reported the application of nanowires for the magnetic control of electrochemical reactivity and demonstrated the modulation of electro catalytic activity by orienting catalytic nanowires at different angles.

In this study, we synthesized Pt–Co/MWCNT catalysts and prepared MEAs with Pt–Co/MWCNT catalysts with magnetic field treatment (labeled M-MEA). The performance of the prepared M-MEA was compared with that of common MEA (labeled C-MEA) without magnetic-field treatment in a single-cell PEMFC. M-MEA and C-MEA were characterized by electrochemical impedance spectroscopy (EIS), cyclic voltammetry (CV), and scanning electron microscopy to determine the changes in the M-MEA that resulted from magnetic-field treatment.

2 Experimental

2.1 Synthesis of Pt–Co/MWCNTs

MWCNTs (98 %, DK nano), $H_2PtCl_6{\cdot}6H_2O$ (99.8 %, Sigma), ethylene glycol (EG, 99.8 %, Sigma), $C_2H_3CoO_2{\cdot}4H_2O$ (99.8 %, Sigma), absolute ethanol (99.8 %, Sigma), and deionized water were used in the experiments. In the modified polyol method, EG was used as a reducing, stabilizing, and dispersing agent. To prepare Co/MWCNT, approximately 100 mg of MWCNT was stirred for 0.5 h after adding a required amount of $C_2H_3CoO_2$ solution (20 mmol l^{-1}). The mass ratio of MWCNT and Co was adjusted to 2:1. After adding ethanol and EG, the mixture was transferred into a three-neck flask and brought to reflux in a water bath. The reflux temperature was controlled at 80 °C, and the pH of the solution was adjusted to 8.5 by adding NaOH. The same procedure was used to synthesize of Pt–Co/MWCNT from Co/MWCNT by adding a required amount of H_2PtCl_6 solution. The mass ratio of Pt, MWCNTs, and Co was adjusted to 2:2:1. After the reaction, the solution was washed, filtered, and dried at 80 °C for 2 h in a vacuum oven. The projected Pt loading of the catalyst was 40 wt %.

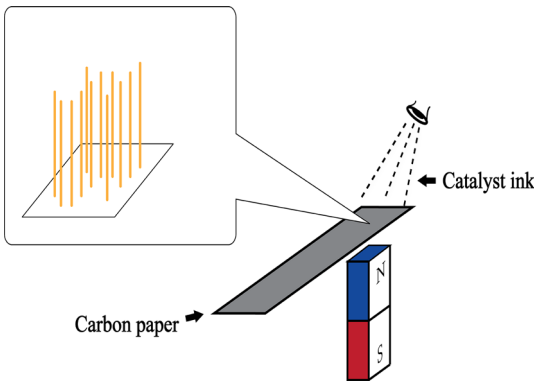

Fig. 1 The experimental setup of preparing MEA with the magnetic field in the *vertical* positions, the catalysts orient parallel to magnetic field *lines*

2.2 MEA preparation

The catalysts were mixed with ethanol and Nafion® ionomer solution (5 wt %, Dupont) in an ultrasonic bath (KUDOS, SK5200LH) at ambient temperature for 30 min to obtain homogeneous catalyst inks. C papers (Toray) were used as diffusion layers. The catalyst inks were separately spread on each of the C paper diffusion layers during treatment with a magnetic field strength of 350 mT, as shown in Fig. 1, under drying at 80 °C for 1 h to form an anodic or cathodic electrode (labeled M-MEA). For comparison, an electrode without magnetic-field treatment was also prepared (labeled C-MEA). Pt loadings of 0.4 mg cm^{-2} were maintained at both the anode and cathode. The effective electrode area was 5 cm^2. MEA was prepared by sandwiching a pre-treated Nafion 212 membrane (Dupont) between the anode and cathode by hot-pressing at 140 °C and 80 bar for 1 min.

2.3 Characterization

Powder X-ray diffraction (XRD) studies were conducted using a PANalytical Empyrean Pro X-ray diffract meter with Ni-filtered Cu Kα radiation as X-ray source. The synthesized catalyst was scanned in a step of 0.016° in the 2θ range from 10 to 90°. The distribution and nanoparticle size of the catalyst were monitored by using a transmission electron microscope (TEM, JEOL 2010) under an accelerating voltage of 200 kV. A TEM sample was obtained by immersing Cu grid coated with C film into the catalyst colloid solution. The grid was then allowed to dry at room temperature. A JEOL-6360LV scanning electron microscope (SEM) was employed to observe the microstructure and morphology of the catalyst layers in MEA.

The electrochemical surface area (ESA) of the cathode in different MEAs was determined by CV (Autolab STAT20, The Netherlands). The cathode was fed with N_2-purged at a rate of 20 ml min^{-1}, where as the anode was fed with 0.1 MPa humidified H_2 at a rate of 40 ml min^{-1} to serve as a dynamic H electrode (DHE). CV curves were obtained by scanning in the range of 0–1.4 V (vs. DHE) at a rate of 50 mV s^{-1}. The integrated peak area of H desorption (0.05–0.4 V vs. DHE) was used to calculate the ESA of the cathode catalysts.

The electrochemical impedance spectra of MEAs were recorded by using a PGSTAT20 potentiostat/frequency response analyzer from Autolab (The Netherlands). The electrochemical impedance spectra of MEAs were recorded under H_2 flow to the anodes of 100 ml min^{-1} to and air flow to the cathodes of 100 ml min^{-1}. Scanning was conducted from high to low frequencies over the range of 10,000–0.1 Hz, with 10 mV amplitude of the sinusoidal potential signal. The measurement was conducted at room temperature and 100 % relative humidity. The electrochemical impedance spectra were analyzed relative to equivalent circuits by using Autolab NOVA version1.8 circuit-fitting software.

2.4 Single cell test

The PEMFC performance of MEAs was tested by using an in-house single fuel cell test set-up. Fuel cell performance was studied at 60 °C and relative humidity of 80 % without back pressure. The stoichiometric ratio of air was 2.5.

3 Results and discussion

Figure 2 shows the XRD pattern of Pt–Co/MWCNTs synthesized by using EG reduction methods. The XRD of Pt–Co/MCNTs shows the hexagonal graphitic peak of MWCNTs corresponding to (002) peak at $2\theta = 25.8°$. The peaks at 39.88°, 46°, 67.16°, and 80.94° were due to Pt(111), Pt(200), Pt(220), and Pt(311) face-centered cubic phases, respectively. The Pt (111) peak shifted to 0.16°. The shift may be attributed to the lattice contraction that occurs when large Pt atoms are substituted by smaller Co atoms. No additional peaks for Co metal or its oxides were observed. These results suggest that Pt and Co species in the Pt–Co catalysts were alloyed [22, 23]. An average crystallite size of 4.26 nm diameter was calculated by using the following Scherrer equation:

$$d = \frac{k\lambda}{B_{\frac{1}{2}} \cos\theta},$$

where d is the average particle size (nm), k is the Scherrer constant (0.89), λ is the wave-length of X-ray radiation (0.15406 nm), and B is the width (in radians) of the diffraction peak at half height [24].

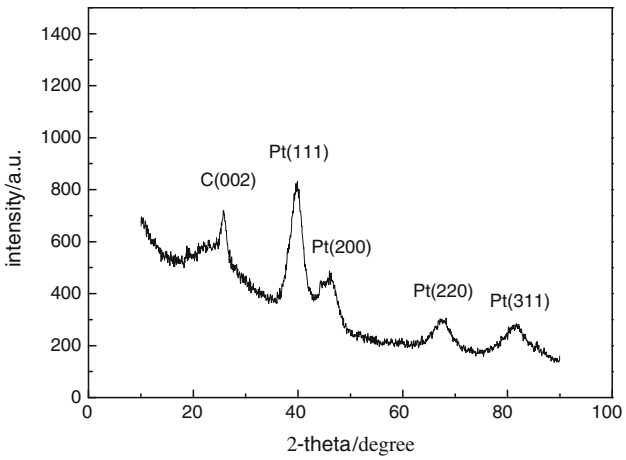

Fig. 2 XRD pattern of Pt–Co/MWCNTs catalysts by modified polyol method

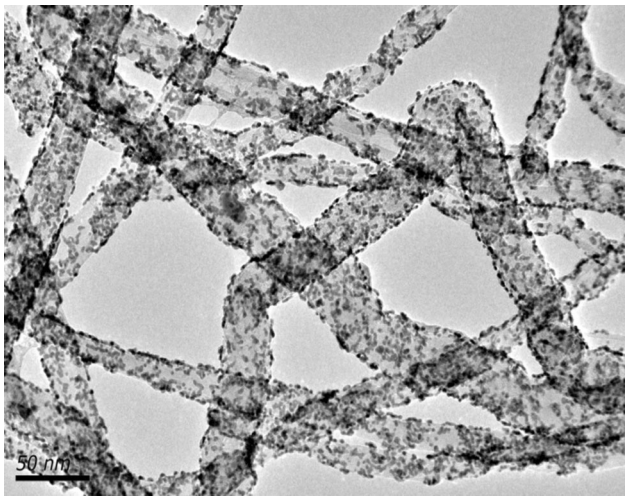

Fig. 3 TEM image of Pt–Co/MWCNTs catalysts by modified polyol method

The morphology and structure of Pt–Co/MWCNTs were explored by using TEM. Figure 3 shows a TEM image of Pt–Co/MWCNTs catalysts. Pt and Co particles were highly dispersed on the MWCNT support. In the EG reduction method, the metal nanoparticles were uniformly distributed with a narrow size because EG functioned as a reducing, stabilizing, and dispersing agent. Figure 4 shows the size distribution of the metal particles. The mean metal particle size was approximately 4 nm, which is in good agreement with the XRD results.

SEM images show noticeable morphological differences between Fig. 5a, b. In contrast to the chaotic catalysts in

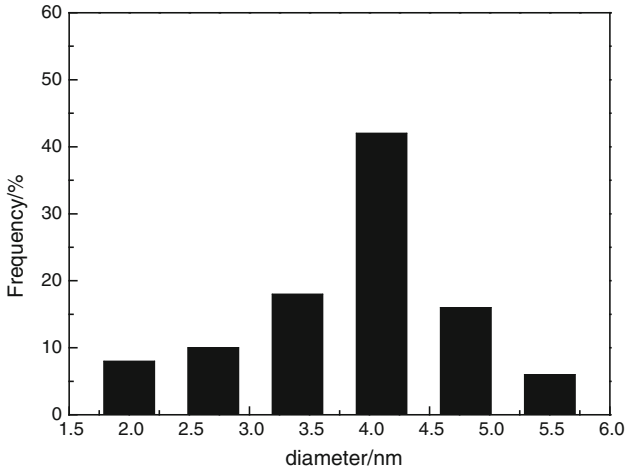

Fig. 4 *Histograms* of the particle size distributions of the catalysts

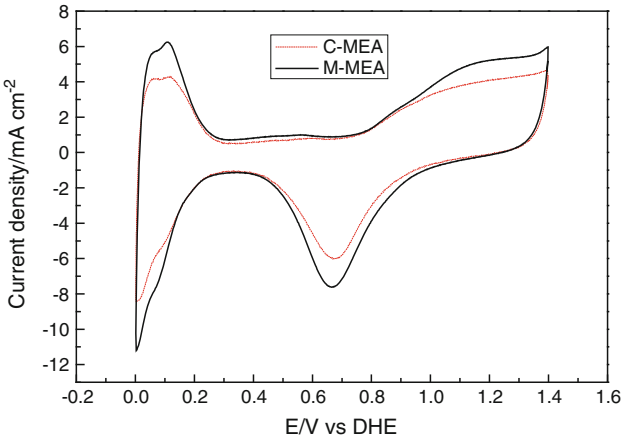

Fig. 6 Cyclic voltammograms of the MEA with the common catalyst layer and the magnetic-field-treated catalyst layer

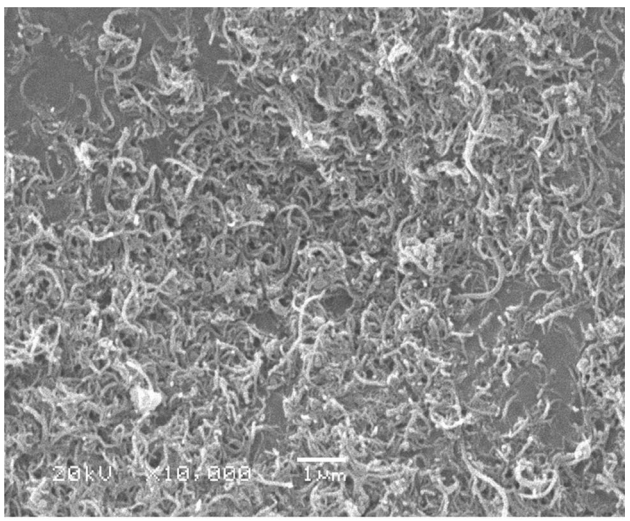

(a)

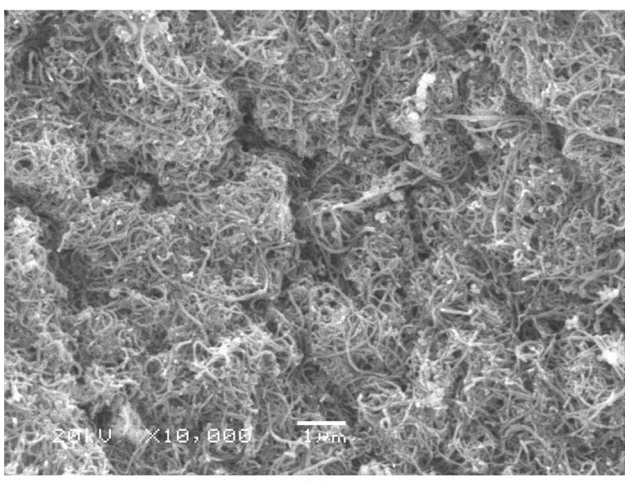

(b)

Fig. 5 SEM images of the common catalyst layer (**a**) and the magnetic-field-treated catalyst layer (**b**)

the common catalyst layer (a), the catalysts in the magnetic-field-treated catalyst layer exhibit "cluster-like structures" (b). The observed cluster distribution of the catalysts in the surface micrograph can be attributed to the aggregation of nanoparticles for magnetic vertical orientation. Co is considered to have ferromagnetism properties. The application of a magnetic field resulted in the rapid magnetization of the catalyst particles and the formation of columns along the field direction through dipolar interaction. This process would continue until all of the solvent has evaporated. Finally, the "cluster-like structure" was frozen.

Two CV curves for M-MEA and C-MEA are shown in Fig. 6. At reduction potentials of −0.40 to −0.10 V, the peak current increased in the hydrogen reduction–adsorption and oxidation–desorption processes. Such increase may be attributed to the following reasons. On one hand, the "cluster-like structures" benefits the charge-transfer process and promotes the hydrogen evolution reaction at the graphite electrode. On the other hand, the magnetic field with certain intensity can affect Pt crystal planes on the basis of the different anisotropy energies of Pt crystal planes in a magnetic field. CV measurements provided direct evidence of an increased ESA for M-MEA as compared with that of C-MEA. With the assumption that the specific quantity of charge for the electro-oxidation of an adsorbed H monolayer on the Pt surface was 210 C cm^{-2} [25], ESA was calculated with the use of the H desorption peaks in the low-potential region between 0.05 and 0.4 V. ESA of 96.8 m^2 g^{-1} was derived for M-MEA, as opposed to 74.65 m^2 g^{-1} for C-MEA. This value indicates an increment of almost 29.6 % in ESA as a result of magnetic-field treatment. The solid-phase aggregates in the vertical direction and the pores in the catalyst layer were increasingly distributed, which caused the increase in ESA.

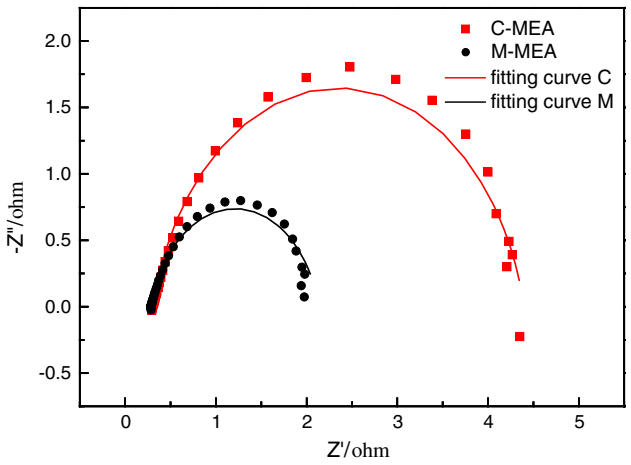

Fig. 7 Electrochemical impedance spectra of MEA with the common catalyst layer and the magnetic-field-treated catalyst layer

Table 1 Calculated values obtained from equivalent circuit

Samples	R_{hf} (Ω)	Error (%)	R_{ct} (Ω)	Error (%)
C-MEA	0.312	4.3	4.09	5.5
M-MEA	0.291	1.4	1.84	2.3

EIS was performed to investigate the characteristics of the proton transfer at the polymer electrolyte membrane and the charge transfer at the catalyst/electrolyte interface. Figure 7 shows the Nyquist plots for the single cell measured at 0.8 V. For all single cells, the Nyquist plots have semicircles with the ohmic resistance (R_{hf}) at the intercept of the x-axis at high frequencies. The charge transfer resistance (R_{ct}) was equivalent to the width of the semicircle. The corresponding equivalent circuits were developed by simulating the impedance spectra using Nova1.8 software. The calculated parameters of the equivalent circuit are listed in Table 1. The R_{hf} values of C-MEA and M-MEA are almost the same. These results can be attributed to the identical catalyst supporter and membrane. However, R_{ct} decreased from 4.09 to 1.84 Ω when MEA was treated with a magnetic field. This result is related to the cluster structure and orientation in vertical direction and is in accordance with the CV result.

MEAs prepared with and without magnetic-field-treatment were compared by testing their V–I polarization curves in PEMFC (Fig. 8). M-MEA exhibited enhanced performance in terms of open-circuit voltage and peak output power density as compared with the C-MEA. Under the same operating conditions, the maximum power density of MEA increased from 149.6 to 223.8 mW cm^{-2}. When C-MEA was replaced by M-MEA, an increase of 49.5 % in peak output power density was achieved. The magnetic-field-treated MEA in the PEMFC presented high voltages

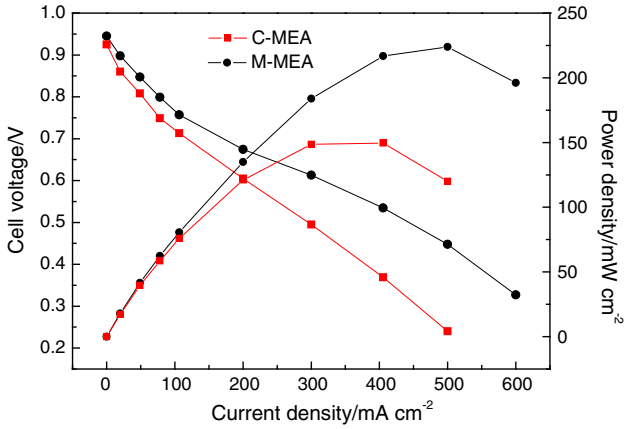

Fig. 8 PEMFC performance curves of single cell with E-MEA and C-MEA; operating temperature = 60 °C; air stoichiometry = 2.5; relative humidity = 80 %

over the whole range of output currents. The enhanced PEMFC performance of M-MEA is consistent with the EIS, SEM, and CV results, which provides evidence of the improved electronic and ionic connections and increased ESA in the magnetic-field-treated catalyst layers.

4 Conclusions

We synthesized Pt–Co/MWCNT catalysts by using the modified polyol method with glycol as reducer, and we obtained uniform nanoparticles. To improve the performance of PEMFC, magnetic-field-treated MEAs were prepared. The enhanced performance of the magnetic-field-treated MEA was verified through PEMFC experiments, which revealed an increase in peak output power density of 49.5 % compared with untreated MEA. The effects of magnetic-field treatment were observed through EIS, SEM, and CV characterizations of MEA. The solid-phase aggregates and the pores in the catalyst layer were increasingly distributed, which resulted in increased ESA and decreased reaction resistance. However, numerous issues and unexplored factors concerning the magnetic-field treatment remain. Further investigation is ongoing in our laboratory.

Acknowledgments This research was funded by the National Basic Research Program of China (973 Program, Grant No. 2012CB215500) and the National Natural Science Foundation of China (No. 21106012).

References

1. Haile SM (2003) Fuel cell materials and components. Acta Mater 51:5981
2. Schultz T, Sundmacher K (2006) Mass charge and energy transport phenomena in a polymer electrolyte membrane (PEM) used in a direct methanol fuel cell (DMFC): modelling and experimental validation of fluxes. J Membr Sci 276:272

3. Yan Xiqiang, Hou Ming, Sun Liyan, Cheng Haibo, Hong Youlu, Liang Dong, Shen Qiang, Ming Pingwen, Yi Baolian (2007) The study on transient characteristic of proton exchange membrane fuel cell stack during dynamic loading. J Power Sour 163:966
4. Antolini E, Salgado JRC, Giz MJ, Gonzalez ER (2005) Effects of geometric and electronic factors on ORR activity of carbon supported Pt–Co electrocatalysts in PEM fuel cells. Int J Hydrogen Energy 30:1213
5. Cho YH, Jeon TY, Lim JW, Cho YH, Ahnb M, Jung N (2011) Performance and stability characteristics of MEAs with carbon-supported Pt and Pt1Ni1 nanoparticles as cathode catalysts in PEM fuel cell. Int J Hydrogen Energy 36:4394
6. Rao CS, Singh DM, Sekhar R, Rangarajan J (2011) Pt–Co electrocatalyst with varying atomic percentage of transition metal. Int J Hydrogen Energy 36:14805
7. Fox EB, Colon-Mercado HR (2010) Effect of pretreatment on Pt–Co/C cathode catalysts for the oxygen reduction reaction. Int J Hydrogen Energy 35:3280
8. Paulus UA, Wokaun A, Scherer GG, Schmidt TG, Stamenkovi V, Radmilovic V (2002) Oxygen reduction on carbon-supported Pt–Ni and Pt–Co alloy catalyst. J Phys Chem B 106:418
9. Mukerjee S, Srinivasan S, Soriaga MP, McBreen J (1995) Role of structural and electronic properties of Pt and Pt alloys on electrocatalysis of oxygen reduction. J Electrochem Soc 142:1409
10. Seo A, Lee J, Han K, Kim H (2006) Performance and stability of Pt based ternary alloy catalysts for PEMFC. Electrochim Acta 52:1603
11. Baglio V, Blasi AD, D'Urso C, Antonucci V, Arico AS, Ornelas R (2008) Development of Pt and Pt–Fe catalysts supported on multi-walled carbon nanotubes for oxygen reduction in direct methanol fuel cells. J Electrochem Soc 155:829
12. Shujuan J, Yanwen M, Guoqiang J, Haisheng T, Xizhang W, Yining F (2009) Facile construction of Pt–Co/CNT nanotube electrocatalysts and their application to the oxygen reduction reaction. Adv Mater 21:4953
13. Oren Y, Freger V, Linder C (2004) Highly conductive ordered heterogeneous ion-exchange membranes. J Membr Sci 239:17
14. Hsiu-Li Lin T, Leon Yu, Han Fang-Hsin (2006) A method for improving ionic conductivity of Nafion membranes and its application to PEMFC. J Polym Res 13:379
15. Schwarz MK, Bauhofer W, Schulte K (2002) Alternating electric field induced agglomeration of carbon black filled resins. Polymer 43:3079
16. Wang HQ, Zhang HY, Zhao WF, Zhang W, Chen GH (2008) Preparation of polymer/oriented graphite nanosheet composite by electric field-inducement. Compos Sci Technol 68:238
17. Wang Z-T, Wang Y-X, Xua L, Gao Q-J, Wei G-Q, Lua J (2009) Electric field-treated MEAs for improved fuel cell performance. J Power Sources 186:293
18. Middelman E (2002) Improved PEM fuel cell electrodes by controlled self-assembly. Fuel Cells Bull 2002:9
19. Yonermura H, Natsuko S, Suyama J, Yamada S (2011) Orientation and organization of gold nanorods on a substrate using a strong magnetic field: effect of aspect ratio. J Photochem Photobio A 220:179
20. Hasanabadi N, Ghaffarian SR, Hasani-Sadrabadi MM (2011) Magnetic field aligned nanocomposite proton exchange membranes based on sulfonated poly (ether sulfone) and Fe_2O_3 nanoparticles for direct methanol fuel cell application. Int J Hydrogen Energy 36:15323
21. Wang J, Scampicchio M, Laocharoensuk R, Valentini F, González-Garcia O, Burdick J (2006) Magnetic tuning of the electrochemical reactivity through controlled surface orientation of catalytic nanowires. J Am Chem Soc 128:4523
22. Xiong LF, Manthiram A (2004) Influence of atomic ordering on the electrocatalytic activity of Pt–Co alloys in alkaline electrolyte and proton exchange membrane fuel cells. J Mater Chem 14:1454
23. Huang QH, Yang H, Tang YW, Lu TH, Akins DL (2006) Carbon supported Pt–Co alloy nanoparticles for oxygen reduction reaction. Electrochem Commun 8:1220
24. Zengcai L, Chengfei Y, Irene A, Rusakova E, Huang D, Peter S (2008) Synthesis of Pt_3Co alloy nanocatalyst via reverse micelle for oxygen reduction reaction in PEMFCs. Top Catal 49:241
25. Lu L, Xu H, Zhao H, Zhu S, Ren R (2012) Investigation of the durability of Pt/C-$RuO_2{\cdot}xH_2O$ catalyst in PEMFC. J Appl Electrochem 42:201